RESEARCH PAPER

CrossMark

A simulation-based study on longitudinal gust response of flexible flapping wings

Toshiyuki Nakata[1] · Ryusuke Noda[2] · Shinobu Kumagai[1] · Hao Liu[1]

Abstract

Winged animals such as insects are capable of flying and surviving in an unsteady and unpredictable aerial environment. They generate and control aerodynamic forces by flapping their flexible wings. While the dynamic shape changes of their flapping wings are known to enhance the efficiency of their flight, they can also affect the stability of a flapping wing flyer under unpredictable disturbances by responding to the sudden changes of aerodynamic forces on the wing. In order to test the hypothesis, the gust response of flexible flapping wings is investigated numerically with a specific focus on the passive maintenance of aerodynamic forces by the wing flexibility. The computational model is based on a dynamic flight simulator that can incorporate the realistic morphology, the kinematics, the structural dynamics, the aerodynamics and the fluid–structure interactions of a hovering hawkmoth. The longitudinal gusts are imposed against the tethered model of a hovering hawkmoth with flexible flapping wings. It is found that the aerodynamic forces on the flapping wings are affected by the gust, because of the increase or decrease in relative wingtip velocity or kinematic angle of attack. The passive shape change of flexible wings can, however, reduce the changes in the magnitude and direction of aerodynamic forces by the gusts from various directions, except for the downward gust. Such adaptive response of the flexible structure to stabilise the attitude can be classified into the mechanical feedback, which works passively with minimal delay, and is of great importance to the design of bio-inspired flapping wings for micro-air vehicles.

Keywords Insect flight · Flapping wing · Flexible wing · Gust response · Fluid–structure interaction · Mechanical feedback

1 Introduction

Insects are capable of flying and surviving in an unsteady, unstructured and unpredictable flow due to disturbances from natural or man-made obstacles and the frictional interaction between the atmospheric winds and the surface of the earth, called the atmospheric boundary layer [1]. Robust and reliable flight of animals in various forms are attracting wide attention from engineers who wish to develop unmanned aerial systems for filming, surveillance and reconnaissance

in a similar environment. A recent centre of attention in the field of animal flight biomechanics is, therefore, the passive and active strategy employed by the animals when they fly under perturbation such as turbulent flow [2, 3], wind gust [4, 5], von Kármán vortex street [6–8], or tornadoes [9].

Unlike conventional aircraft, small winged animals, such as insects, move their wings back and forth in order to generate aerodynamic force, changing their angle of attack dynamically. Therefore, their flight heavily relies on the various unsteady aerodynamic mechanisms such as leading-edge vortex (LEV), rotational circulation and drag, and wake capture [10–13]. Because of such unsteadiness, the flapping wing is suggested to be able to avoid drastic stall even in the heavy turbulence [14]. Insect flapping flight is, therefore, thought to possess inherent robustness against the unpredictable disturbances.

However, insect flight, especially when hovering, is known to be dynamically unstable [15, 16]. In order to cope with such instability, they hold a redundancy for the control

✉ Toshiyuki Nakata
 tnakata@chiba-u.jp

✉ Hao Liu
 hliu@faculty.chiba-u.jp

1 Graduate School of Engineering, Chiba University, Chiba 263-8522, Japan

2 Department of Mechanical Engineering, Kanto Gakuin University, Kanagawa 263-8501, Japan

of aerodynamic forces to manoeuvre via tuning of their wing kinematics [15, 17]. Insects must respond to their instability or external disturbances so as to maintain their state by a neural feedback loop that utilizes the sensory input from organs such as eyes or halteres. Such active mechanisms for maintaining their state or switching flight mode are widely employed even in man-made mechanical systems because of its utility, but, in insect flight, they comes with sensory delay that has an influence on the flight performance [18].

Compared to our mechanical systems, winged animals can be characterized by their structural flexibility. Flapping wings of insects must be light to reduce the inertial power for flapping and, therefore, are inevitably thin and flexible. The arrangement of the wing vein and membrane allows the wing to deform in a particular way [19]. The interaction of the wing structure, aerodynamic and inertial forces passively determines the wing deformation and hence the aerodynamic performance of flexible flapping wings [20, 21]. Several studies suggested that the wing deformation, such as bending and twisting, can enhance their flight efficiency [21–25].

The flexibility in flapping wings may be able to ease the control against the unpredictable disturbances, because the flexible wing can respond to the aerodynamic disturbances passively. The passive response may reduce the unfavourable changes in aerodynamic forces. This passive mechanism, classified into the mechanical feedback loop [26], can respond with minimal latency, since it does not require any transduction or processing. Running cockroaches utilize mechanical feedback to make neural feedback control simpler [27]. The underwing coverts of a steppe eagle are suggested to be an aeroelastic device for high-lift generation and passive flow control [28]. Bumblebees are suggested to utilize active neural feedback to manoeuvre at lower frequencies and a passive mechanism to cope with perturbations at higher frequencies in unsteady complex airflows [29]. Wing deformation can improve the flight stability, which is suggested through an experiment of bumblebees in turbulence with stiffened wings [30].

In order to mitigate the effect of disturbances passively, flapping wings must respond at high frequency, at least at the wingbeat frequency even against the spatially uniform gust, since the flapping wing changes its attitude dynamically. The measured resonance of insect wings suggest that this response is possible. The wingbeat frequency of dragonflies was found to be 16% of the natural frequency of their wing [31]. Similarly, the wingbeat frequency of the flapping wings of eight insect species, measured by Ha et al. [32], are lower than the resonance of the wing except for Hymenoptera. These results suggest that their flapping wings cannot enhance the aerodynamic efficiency through resonance. However, since the flexible structure can respond to the external force with small delay if its frequency is much lower than the resonance, the insect wings can respond to, and may reduce, the sudden change in aerodynamic force at their wingbeat frequency.

In this study, in order to test the hypothesis that the flexible flapping wings can mitigate the effect of the gust passively through its deformation, we investigated the gust response of flapping wing flyers computationally with a specific focus on passive wing deformation in response to wind gust. We have utilized the numerical model for a hovering hawkmoth with flexible wings constructed in a previous study [33]. The gust is assumed to be spatially larger than the flapping wing and is modelled by a smoothed step function given to the flyer from longitudinal eight directions. The gust response of the flapping wings is evaluated in terms of the relative changes in the force magnitude and angle, and pitching torque.

2 Method

2.1 Integrated model of a hovering hawkmoth with flexible wings

In order to model a hovering hawkmoth with flexible flapping wings, we have employed a bio-inspired dynamic flight simulator that can incorporate the realistic morphological, kinematic, structural and fluid dynamic models, and fluid–structure interactions [33, 34]. The morphological model of a wing is constructed by tracing the outline of the wing of a hawkmoth, Agrius convolvuli. A flyer is modelled by the multi-blocked overset grid method in which the left and right wings were modelled separately as different local blocks with a body grid as a global grid to give outer boundary conditions for local wing blocks shown in Fig. 1a. The kinematic model, defined in Fig. 1b, is constructed by simplifying the measured kinematics of a hovering hawkmoth [35]. In order to avoid artefact due to the impulsive start of the wing motion, the wing kinematics is weighted by an exponential function (Fig. 1e) so that the wing angles, as well as the simulated aerodynamic forces and torques, gradually increases and converges after three wingbeats (Fig. 1e–g). The parameters used in this study are listed in Table 1.

A fortified Navier–Stokes solver for the dynamically moving multi-blocked overset-grid system [34] is employed to model the flapping wing aerodynamics in this study. The governing equation of CFD simulator is the unsteady, three-dimensional and incompressible Navier–Stokes equations. The simulator is validated by the comparisons against the variety of experimental results. The details can be found in the previous studies [33, 34]. The CSD simulator is based on a finite element method that combines Allman triangular element and discrete Kirchhoff triangular element with an anisotropic structure. The elements are utilized to model the nonlinear dynamic response by introducing an
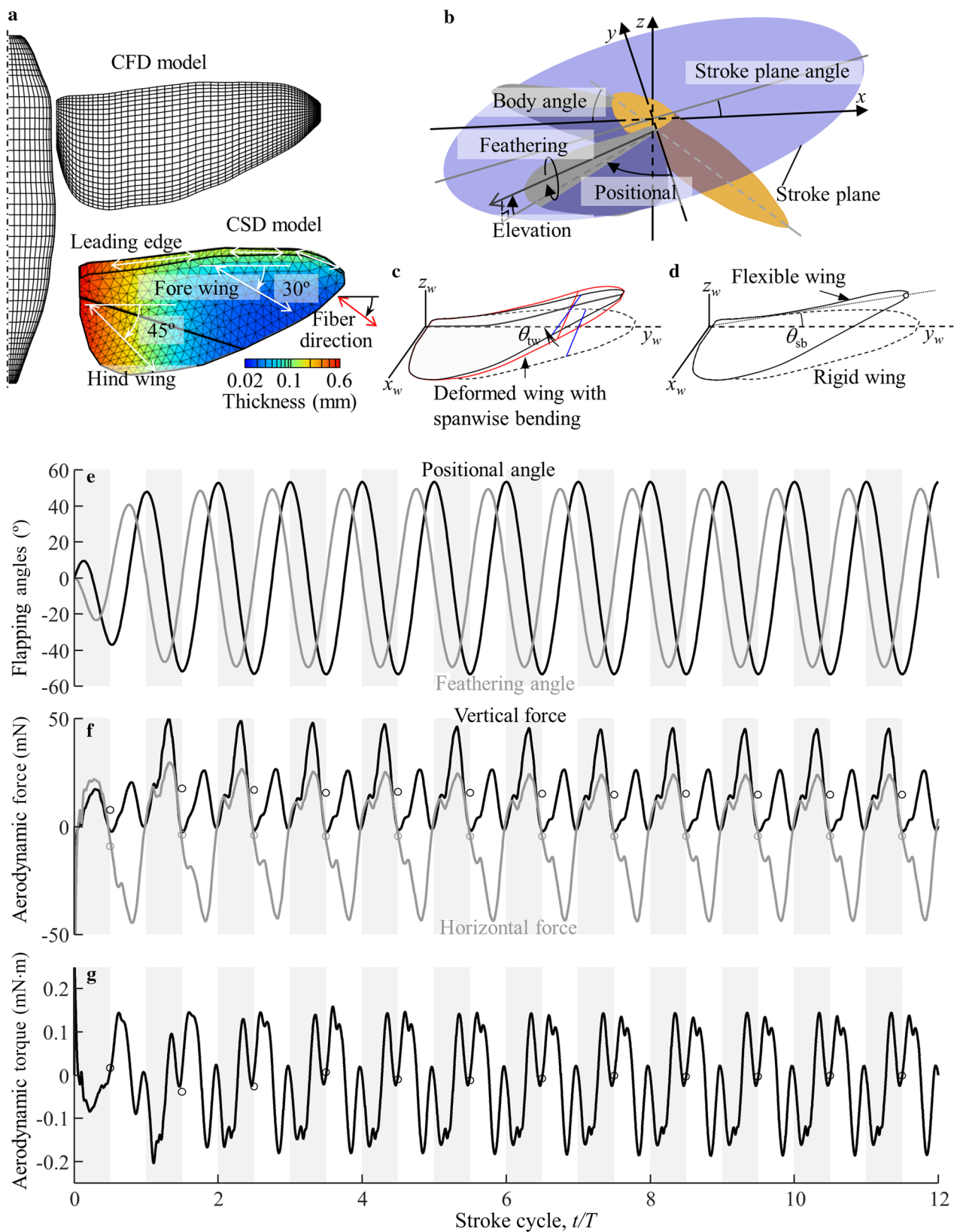
Fig. 1 Computational model. **a** Morphological and structural models for computational fluid dynamic (CFD) and computational structural dynamic (CSD) analyses of a hawkmoth. **b** Definition of coordinate systems and flapping angles. **c** Definition of wing twist. **d** Definition of spanwise bending. **e** Time-series of the positional (black) and feathering (grey) angles. **f** Time-series of the vertical (black) and horizontal (grey) forces. **g** Time-series of the pitching torque of rigid wing without gust (the shaded area corresponds to the downstroke)

Table 1 Parameters for computational fluid dynamic analyses

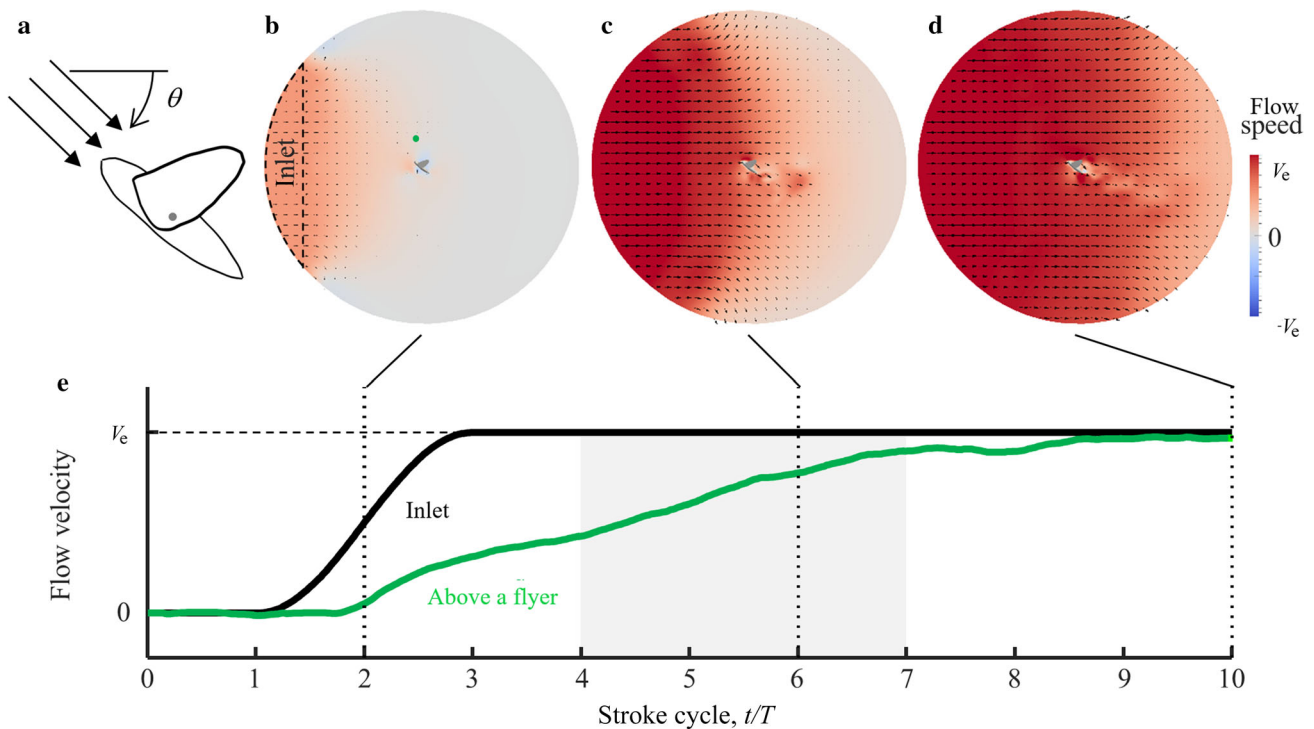| Wing length (mm)	Mean chord length (mm)	Wing beat frequency (Hz)	Wing beat amplitude (rad)	Reynolds number	Reduced frequency	Grid	Non-dimensional time step
50.5	18.3	26.1	2	6300	0.3	$45 \times 65 \times 25$ (wing) $45 \times 43 \times 65$ (body)	0.01

Fig. 2 Gust model. **a** Definition of gust direction, grey dot indicates the position of centre of mass. Flow field at sagittal plane of a hawkmoth after **b** 2 wingbeats. **c** 6 wingbeats. **d** 10 wingbeats. From the onset of the simulation with the frontal gust. **e** Time-series of the horizontal flow velocity at inlet and a probe above a flyer shown in **b** (the shaded area corresponds to the downstroke)

updated Lagrangian formulation. The structural model has an anisotropy and thickness distribution (Fig. 1a) and is validated by the comparison against the measured deformation of a rotating hawkmoth wing [36]. CFD and CSD simulators were combined by a loose coupling method to simulate a three-dimensional, nonlinear and dynamic fluid–structure interaction. The grid and time step refinement of the current model were performed in the previous study [36].

The simulated wing deformation is quantified by the wing twist and the spanwise bending. The twist is defined as the rotation of each cross section about the spanwise axis, and the twist at 80% of the wing length from the wing base is used as a representative value (Fig. 1c). The spanwise bending angle is defined as the elevation of the wing tip normal to the surface of rigid wing (Fig. 1d).

2.2 Gust response

Flyers can be translated and rotated without neural control under gust. In this study, however, the flyer is tethered in the computational space throughout the simulation. The assumption is thought to be reasonable since the time-scale of the body dynamics tends to be larger than the flapping wing motion. Moreover, it is very important to evaluate the gust effect on the flapping wing aerodynamics at the very beginning of the body motion. The gust is imposed into the computational domain by smoothly increasing the flow speed at inlet of computational domain. The inlet is set to be at 20 mean chord lengths away from a flyer so that the artificial increase of the flow speed does not cause any artefact in the vicinity of the flyer. In order to avoid unnaturally sharp and sudden increase of the flow speed and to simulate more realistic gust, the flow velocity follows the smoothed step
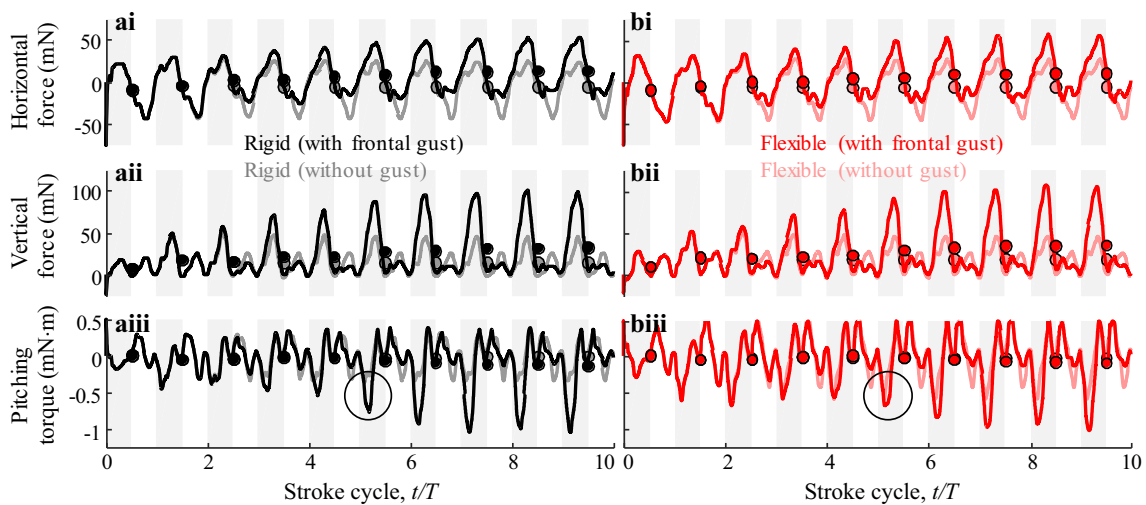
Fig. 3 Time-series of (i) horizontal forces, (ii) vertical forces, and (iii) pitching torques on: **a** rigid wing with gust, **b** flexible wing with gust (grey and pink lines are the forces or torques without gust. The shaded area corresponds to the downstroke)
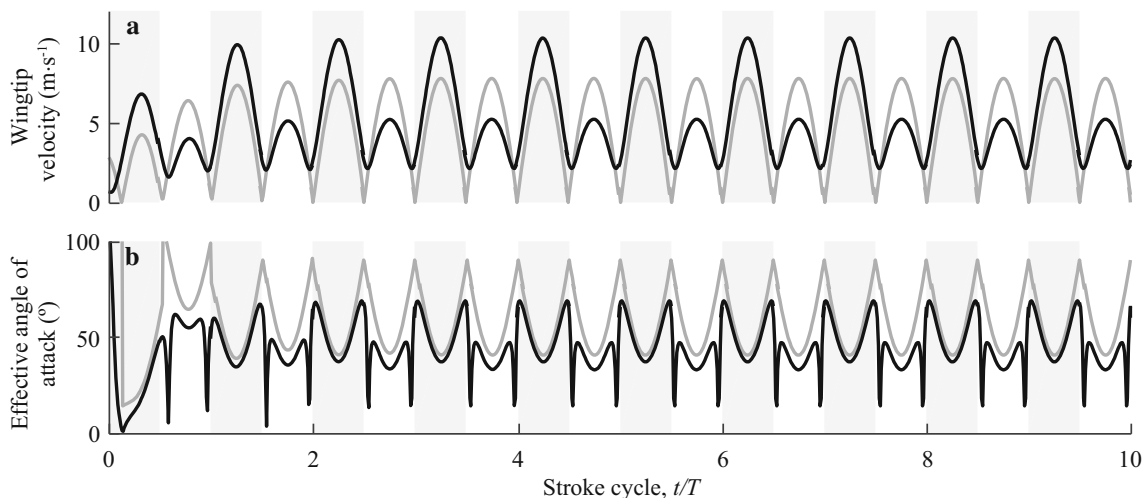

Fig. 4 **a** Time-series of the relative wingtip velocity of rigid flapping wing with (black) or without (grey) gust. **b** Kinematic angle of attack of rigid flapping wing with (black) or without (grey) gust

function and reaches the terminal velocity in two wingbeats at the inlet (black line in Fig. 2e). Hawkmoths were found to be able to fly at 3 m/s with von Kármán vortex street [7]. The gust in this study does not contain such disturbances, but the intensity of the gust at which hawkmoths can respond without falling may not be too far from the speed. Therefore, the terminal velocity (V_e) of the gust is set to be 50% of the mean wingtip velocity (2.6 m/s). As can be seen from Fig. 2b–d, which shows the flow development under frontal gust, the gust can be assumed to be very large-scale compared to the flyer. The outlet boundary condition is used for the external boundary except for the inlet. Therefore, as can be seen in Fig. 2b–d, the flow goes out at the boundary so as to maintain the incompressibility in the domain. The time-course of the

flow velocity at the flyer is measured by a virtual probe at 5 mean chord lengths above a flyer, which can be assumed to be far enough to ignore the effect of the induced flow by the flapping wings (green dot in Fig. 2b). As shown in Fig. 2e, the flow propagates toward the flyer and starts to reach after two wingbeats from the onset of simulation. Therefore, the gust effect can be evaluated when the flow and the wing deformation are close to those without gust. The flow is fully developed after 10 wingbeats. The effect of the gust direction is further investigated by imposing the gust from the various direction. The angle of the gust, θ, is measured from the front in a clockwise direction (Fig. 2a).

The longitudinal gust response is evaluated by the changes in the magnitude and the direction of aerodynamic force and
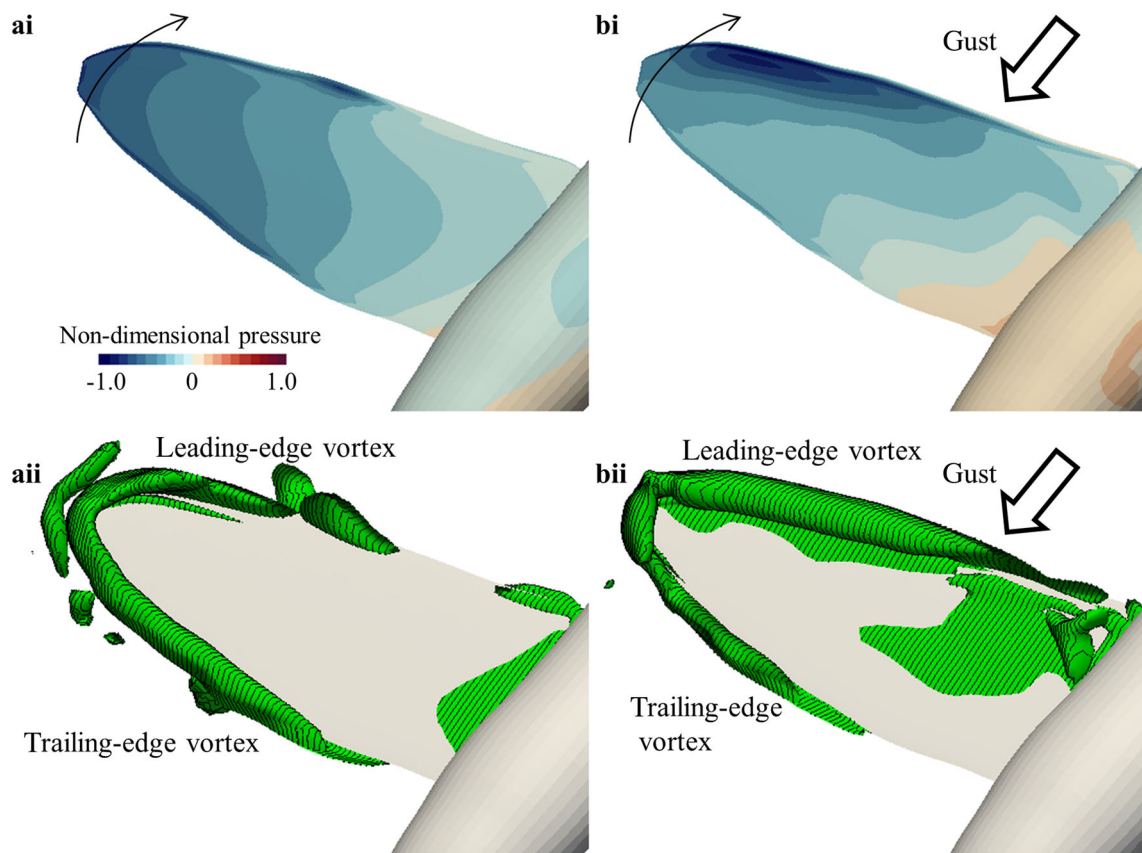
Fig. 5 (i) Pressure on the wing surface and (ii) iso-Q surface around the rigid flapping wings during pronation of 5th cycle. **a** Without gust, **b** with gust

the pitching torque in comparison with the forces and torques without gust. The wingbeat frequency of insect flapping wing is relatively higher than the natural frequency of the insect body. The dynamic changes of forces and torques due to the flapping can then be neglected when discussing the dynamics of flapping wing flyers as proposed in previous studies on the flight stability [37, 38]. Therefore, we mainly focused on the cycle-averaged forces and torques in this study. The changes in forces and torques due to the gust are quantified by the relative increase of the force magnitude and the pitching torque, σ, as follows:

$$\sigma = \frac{\bar{F}_g - \bar{F}}{\bar{F}},$$

where $\bar{F}_g$ and $\bar{F}$ are the force magnitude or the pitching torque with and without gust, respectively. The overbar represents an average over a single wingbeat. The force magnitude is calculated from the cycle-averaged horizontal and vertical forces. The absolute mean was used for the cycle-average of pitching torque. The change in the force direction is further evaluated by the angle between the cycle-averaged aerodynamic force vectors with and without gust.

For further discussion, we have tested another artificial wing model with the prescribed deformation that keeps the twist and the spanwise bending of the flexible flapping wings without gust. For prescribing the wing shape, the twist and the spanwise bending, β, was separately interpolated by fifth-order polynomials spatially, and fifth-order Fourier series temporally, as follows:

$$\beta = \sum_{i=0}^{5} \sum_{j=0}^{5} \hat{r}^i \left[a_{i,j} \cos(j\omega t) + b_{i,j} \sin(j\omega t) \right],$$

where $\hat{r}$ is the spanwise position of the wing normalized by the wing length, $a_{i,j}$ and $b_{i,j}$ are the Fourier coefficients, and ω is the angular frequency.

3 Results

3.1 Frontal gust response of rigid and flexible flapping wings

We first see the details of the gust response of the rigid and flexible flapping wings under the frontal gust ($\theta = 0°$). Figure 3 shows the time-series of horizontal and vertical forces, and pitching torque of rigid (black and grey) and flexible
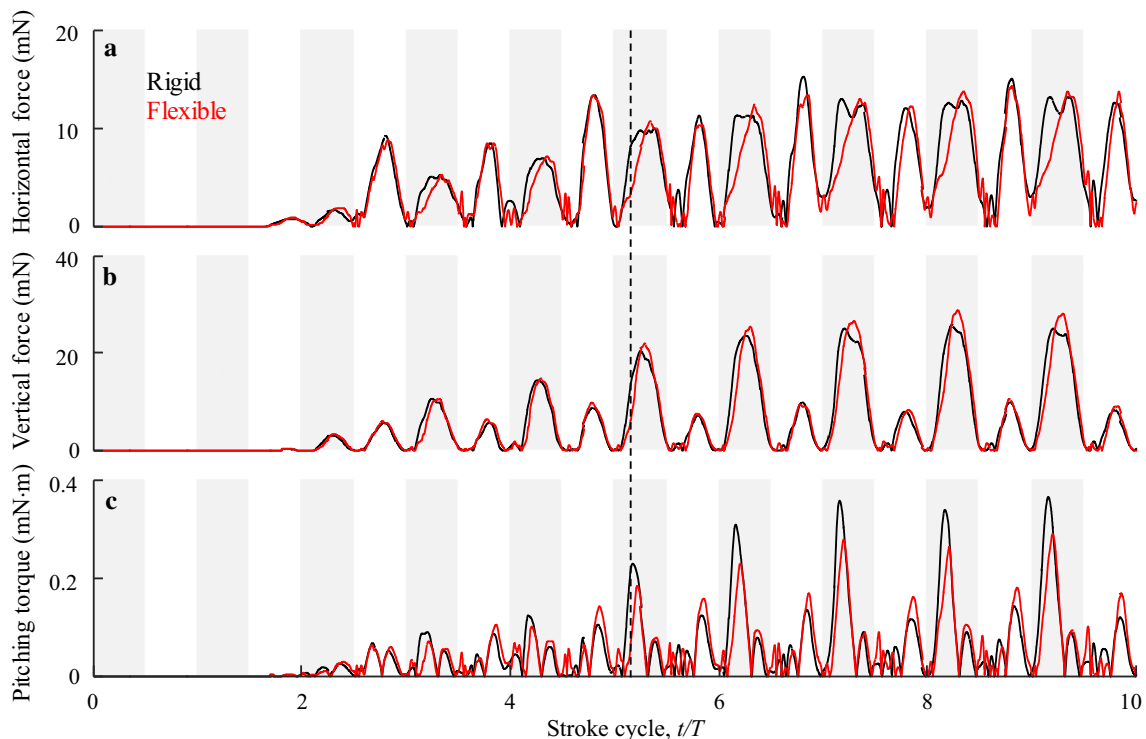
Fig. 6 Time-series of the differences between forces, or torques with and without gust. **a** Horizontal forces, **b** vertical forces, **c** pitching torques with and without gust (vertical broken line indicates the time instant for the visualization in Fig. 7. The shaded area corresponds to the downstroke)

(red and pink) wings with (black and red) or without (grey and pink) frontal gust ($\theta = 0°$). The cycle-averaged forces and torques are shown by the filled circles. Both rigid and flexible wings respond to the frontal gust in a similar manner; the horizontal force shifts backward (in positive x) after 3rd cycle, and the vertical force is increased during downstroke, while it is decreased during upstroke (Fig. 3ai, aii, bi, bii). These changes are thought to be due to the increase or decrease of the relative wing velocity and the kinematic angle of attack [39]. Figure 4 shows the relative wingtip velocity and the kinematic angle of attack of rigid flapping wings with or without frontal steady flow (2.6 m/s). It can be confirmed that the relative wingtip velocity is increased during downstroke and decreased during upstroke. The kinematic angle of attack, which is defined as the attitude of the wing against the relative wind, is decreased throughout the whole wingbeat, but the changes are clearer during upstroke. The increase of the vertical force during downstroke exceeds the decrease of the vertical force during upstroke, because the aerodynamic forces are proportional to the square of the velocity. The mean vertical force is, therefore, increased in comparison with the force without gust. The gust effect on the pitching torque is substantial from pronation to downstroke (Fig. 3aiii). The pressure and iso-Q surface around the wing at the beginning of the downstroke (5th cycle) of rigid wing with and without gust are illustrated in Fig. 5. Because there is a frontal

gust, the leading-edge vortex is quickly built up on the wing (Fig. 5bii), while the leading-edge vortex is still quite weak on the wing without gust at the same time instant (Fig. 5aii). The leading-edge vortex accounts for the strong negative pressure on the wing (Fig. 5bi) and, therefore, large negative (nose-down) pitching torque around the centre of mass (grey dot in Fig. 2a) at the time instant.

The frontal gust responses of the flexible wings is qualitatively similar to the rigid wing (Fig. 3b), while there are quantitative discrepancies due to the wing flexibility. For example, the cycle-averaged pitching torques are relatively unchanged while those of rigid wings are increased by the frontal gust (circles in Fig. 3aiii, biii). In order to highlight the differences of gust response between rigid and flexible wings, the time-series of the instantaneous differences between the forces or the torques with or without gust are plotted in Fig. 6. While the rigid and flexible wings respond to the gust indifferently during upstroke, it can be seen that the force differences of flexible wings are lower than that of rigid wings at early downstroke. The pressure contours on the upper surface of the wing at the time instant (vertical broken line in Fig. 6) are compared in Fig. 7. The strong negative pressure around the leading edge is induced by the leading-edge vortex. While the negative pressure area on the rigid wing is strengthened and widened by the gust (Fig. 7ai, aii), the difference caused by the frontal gust is marginal in
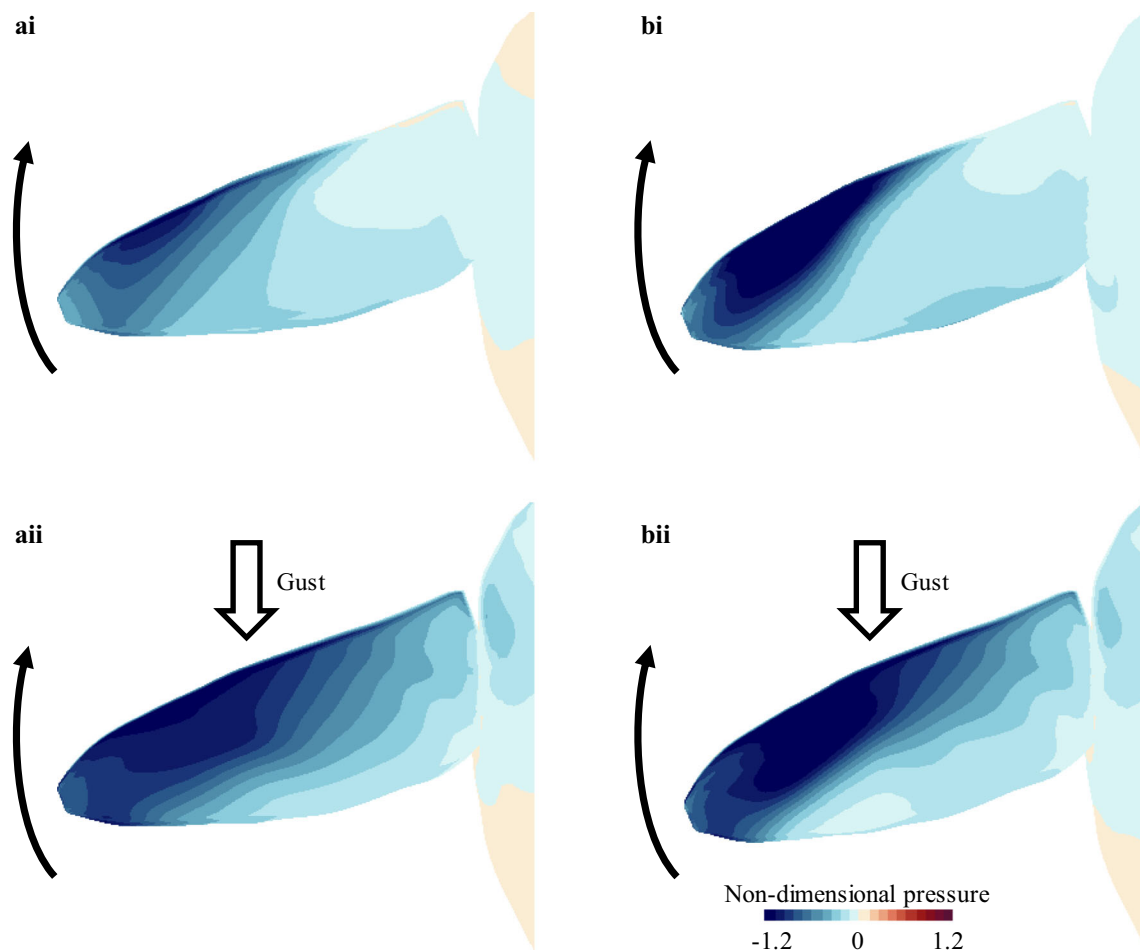
Fig. 7 Pressure distribution on the surface of at middle of the downstroke (i) without, (ii) with gust. **a** Rigid wings, **b** flexible wings

case of the flexible wings (Fig. 7bi, bii). The time-series of the wing deformation of the flexible wing with and without gust are plotted in Fig. 8. The twist and the spanwise bending are affected by the frontal gust because of the flexible wing's capability to passively change its shape in response to the gust. The adaptive shape change affects the speed of translational and rotational motion especially at early down stroke (Fig. 8c, d; vertical line with highlight by circles). The changes in the velocities account for the difference in the gust response between rigid and flexible wings shown in Fig. 7. While such mechanism may not work at much higher wind speed because of the redundant deformation, we have confirmed that the gust effect in terms of the relative increase of forces and torques, and the difference of the angles can be reduced by the wing flexibility at different speeds up to 62.5% of the mean wingtip velocity (3.25 m/s) as can be seen in Fig. 9.

3.2 Gust response of flapping wing

In this section, we focus on the cycle-averaged forces and torques in order to see the general responses of rigid and flexible flapping wings against the longitudinal gust from various directions. The vectors of aerodynamic forces averaged at the 6th cycle are illustrated in Fig. 10. The forces by both rigid and flexible wings (black and red) were bent toward the downstream of gust except for 225° and 270°. While the magnitudes (length) are varied in a similar way, the directions of the vectors by the flexible wings in response to the gust are closer to the vectors without gust (red and black at the centre or thinner vectors) than those of rigid wings in all of the gust directions. This is thought to be favourable when the flyer faces at the gust because, if the force direction is unchanged, the flyers' attitude may be maintained longer without control.

The time-series of the relative increase of the cycle-averaged force magnitude, the angles between the cycle-averaged force vectors with and without gust, and the relative
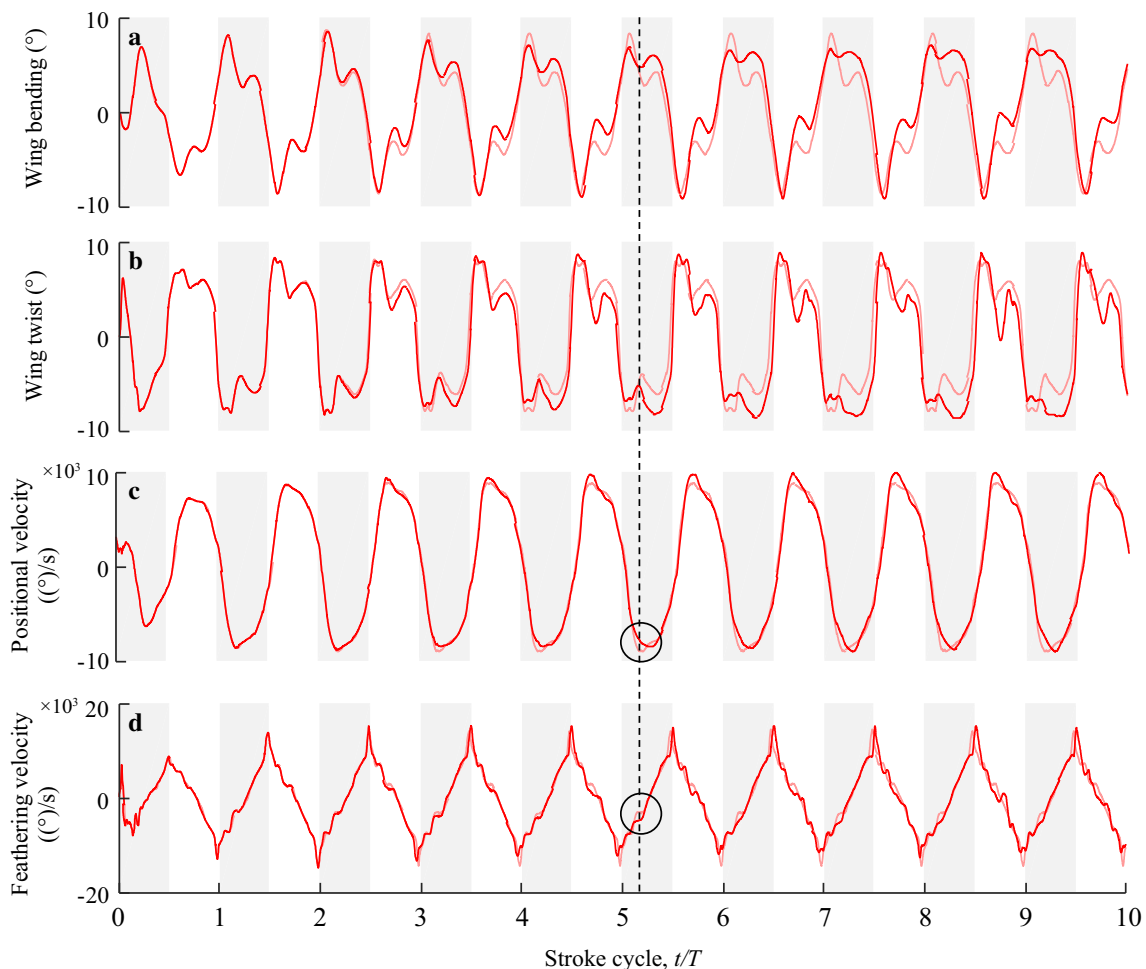
Fig. 8 Time-series of the wing deformation of flexible wings with (red) or without (pink) gust. **a** Wing bending, **b** wing twist, **c** positional angular velocity, **d** feathering angular velocity (the shaded area corresponds to the downstroke)

increase of the pitching torque are plotted in Fig. 11. It can be seen that the effect of the gust is increased with increasing the wingbeat cycle, and hence the wind speed (see Fig. 2). The changes in the force magnitude and direction are relatively low at 270° (upward gust), which is probably because the downwash from the flapping wings can mitigate the effect of the upward gust. The changes in force directions are relatively smaller in flexible wings (red) than those in rigid wings (black), which can also be seen from Fig. 10. The gust effects on the force magnitude and torque of flexible wings are lower than those of rigid wings for most of the cases except for the gust from 45° to 90° (downward gust), especially when the wind speed is higher (6th and 7th cycles). In most of the cases except for the gust from 45° to 90°, the flapping wings with prescribed deformation (green lines in Fig. 11) are also less sensitive to the gust than the rigid wings. The difference between the flexible wings and the wings with prescribed deformation is relatively small, but, in most of the cases except for the gust from 45° to 90°, the changes

in forces or torques of flexible wings are smaller than those of the wings with prescribed deformation. Such insensitivity of the flexible wings to the gust are thought to be due to the passive deformation in response to the gust, as discussed for frontal gust in the previous section.

4 Discussion

The gust used in this study can be considered large scale. The gust reaches steady state after about 10 wingbeat cycles without noticeable spatial distribution in streamwise plane. The terminal wind speed is the half of the mean wingtip velocity, and can be assumed as a relatively strong gust. From the detailed investigation of the force changes due to the frontal gust, the effect of the gust can be fairly explained by the relative wingtip velocity and the kinematic angle of attack, implying that, unlike the conventional fixed wing aircraft, the gust with the strength in this study does not affect the flapping
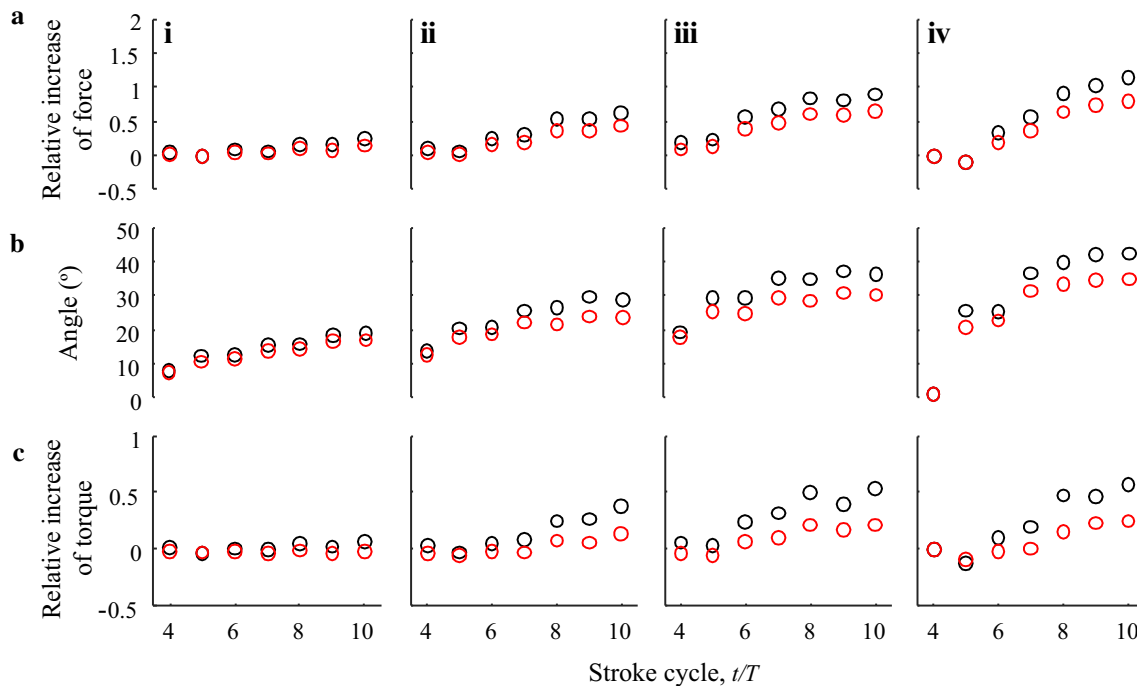
Fig. 9 Time-series of the relative increase on the rigid (black) and flexible (red) wings under the frontal gust with the terminal velocities of (i) 25%, (ii) 37.5%, (iii) 50%, and (iv) 62.5%. **a** Cycle-averaged force magnitude, **b** angle between the cycle-averaged force vectors with and without gust, **c** absolute mean of pitching torque

wing aerodynamics drastically because of the unsteadiness in flapping wing as suggested for the flapping wing in heavy turbulence [14].

Flexible wings are found to be able to mitigate the gust effect from various directions (except for downward gust) in this study. We expected two mechanisms of gust mitigation by the wing flexibility. Firstly, there may be a shape favourable to the gust rejection, which is evident from the good performance of the wings with prescribed wing deformation (green lines in Fig. 11). The shapes of those wings are time-varying, but fixed artificially, and it can mitigate the gust effect up to the similar level of flexible wings under several conditions. Mistick et al. [30] found that the wing flexibility improves the flight stability of bumblebees by reducing the projected surface area with respect to the flow, which imply that the wing shape is very important to mitigate the effect of disturbances. We further suggest that the wing can change its shape under gust by its flexibility, which can help to cancel the changes in relative wing velocity and the kinematic angle of attack. We could confirm the insensitivity of the suction by leading-edge vortex on the flexible wing (Fig. 7), and the better performance of the flexible wings compared to the wings with prescribed deformation in most cases (Fig. 11). There may be a limit on the function of such mechanism, since the insect wing can be assumed as a single plate unlike the bird

wing with feathers that can respond to the relatively small disturbances locally [28]. In this study, we demonstrated the effectiveness of the adaptive bending or twist of the whole wing structure in terms of the mitigation of the gust in relatively large scale. It should be noted that the prescribed deformation also changes the wing shape dynamically, but such shape change is difficult to achieve without the passive wing deformation.

The flexible wing performs worse under downward gust. In order to clarify the mechanism of the high sensitivity of the flexible wings under the gust from 45° to 90°, the kinematics of the cross sections at 80% of wing length from wing base under the frontal ($\theta = 0°$) and downward ($\theta = 90°$) gust are plotted in Fig. 12. It is seen that the wing deforms more during downstroke and less during upstroke under frontal gust. On the other hand, in case of the downward gust, the shape change due to the gust is relatively smaller especially during upstroke as can be seen by the comparison between the cross sections of flexible wings with and without gust (Fig. 12). Such suppression of the passive response is thought to be due to the vertical force for weight support that is in opposition to the force due to the downward gust. The relative changes in forces or torques due to the downward gust can, therefore, be increased by the flexible wings, which is inevitable as long as flapping wings generate vertical forces.
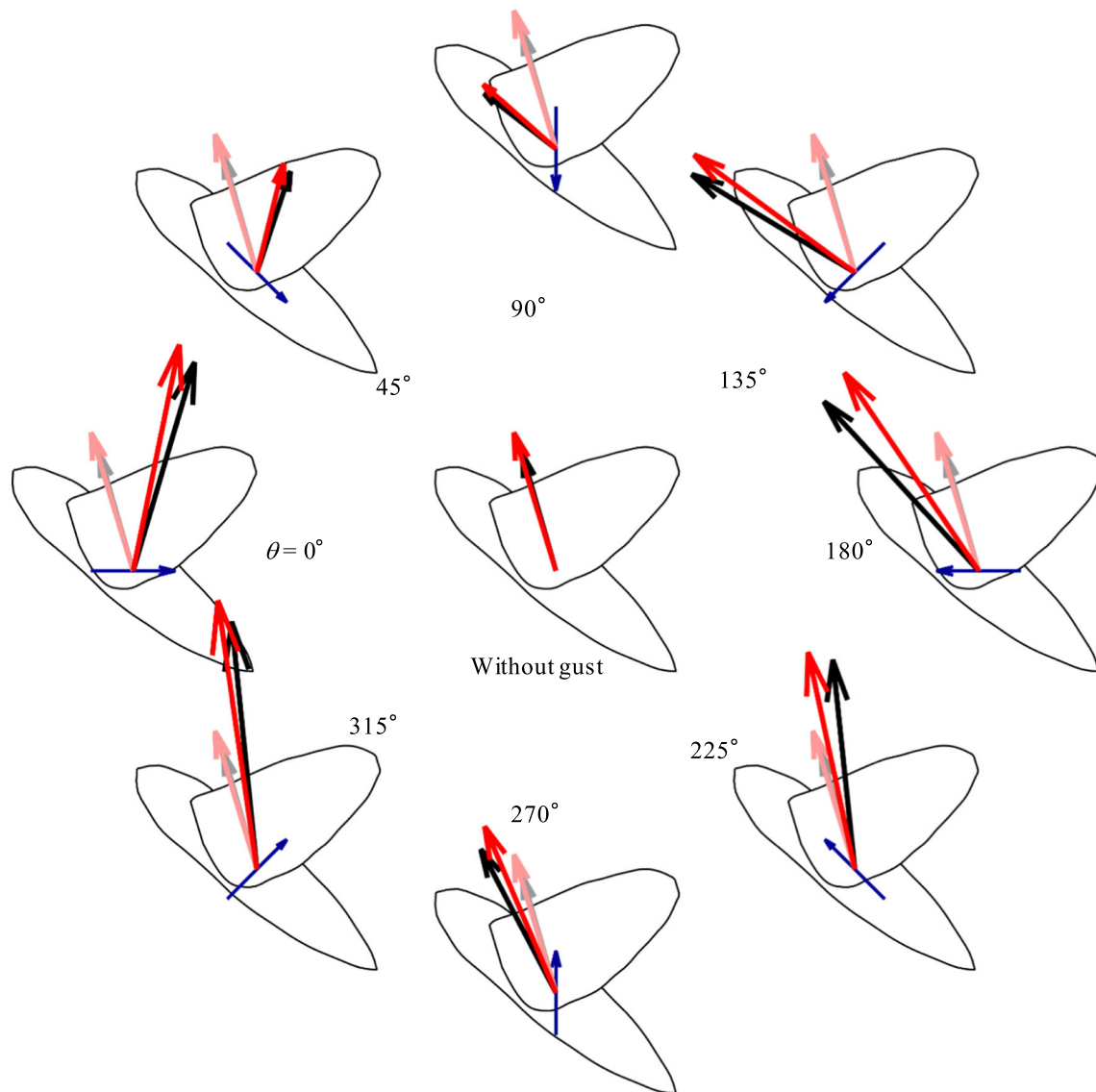
Fig. 10 Effect of gust direction (blue arrows) on the cycle-averaged force vectors by rigid (black) and flexible (red) flapping wings (thinner vectors represents the cycle-averaged force vectors of rigid and flexible flapping wings without gust)

The higher sensitivity to the downward gust is a clear disadvantage of the flexible wing and must be taken into account when designing micro air vehicle. Gusts in the natural world, however, may not contain such vertical components in the three-dimensional gust. Most of the animals fly within the atmospheric boundary layer that is affected by the friction with the ground and ranges from the ground to between 100 m and 1000 m [1]. Turbulence intensity, for example, is found to be lower in vertical direction than in longitudinal or lateral direction, according to the measurements on a moving vehicle [1]. While there is no clear experimental evidence, it is reasonable that the vertical component of the gust is attenuated when the flyer approaches to the ground [1].

The passive shape change in response to the external disturbances, and its ability to mitigate gusts, is particularly important for aerial animals and unmanned aerial systems, since it is extremely difficult to predict oncoming disturbances such as gusts in air. Gust mitigation through passive wing deformation can be classified into a mechanical feedback loop, which, unlike the neural feedback loop, can respond to the disturbances without large delay [26]. The neural feedback loop is necessary for animals or manmade systems to achieve stable flight in air and switch the flight mode, but the mechanical feedback loop can facilitate the control under unpredictable environment by mitigating the instability. Because of the lack of direct measurement, we cannot conclude that winged animals such as hovering hawk-
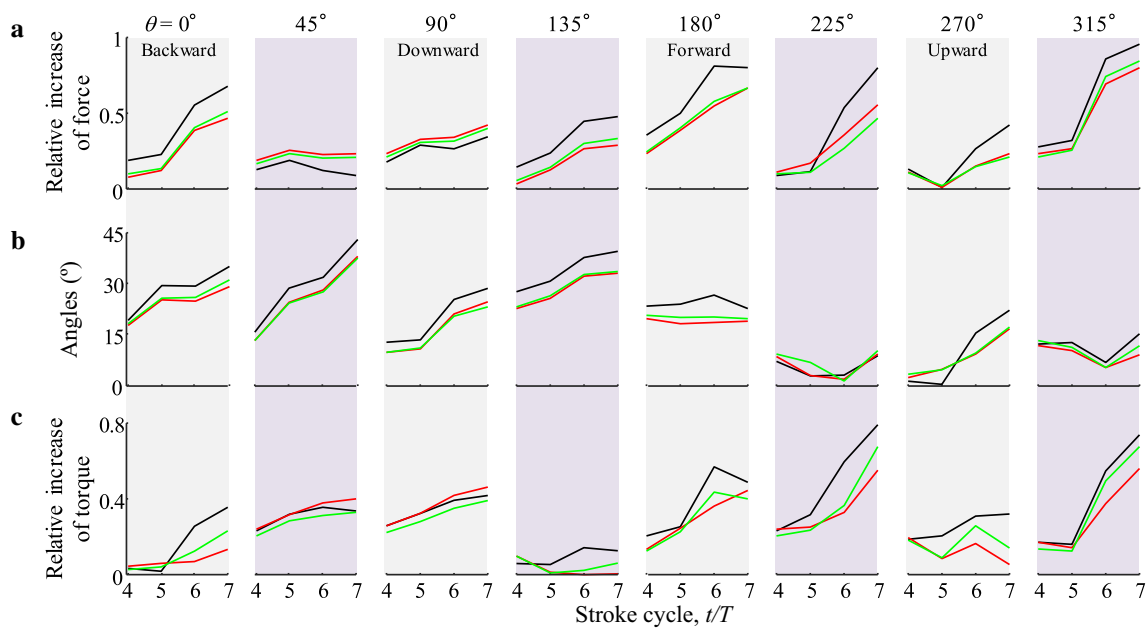
Fig. 11 a Time-series of the relative increase of cycle-averaged force magnitude. **b** Time-series of the angle between the cycle-averaged force vectors with and without gust. **c** Time-series of the relative increase of the absolute mean of pitching torque on the rigid (black) and flexible (red) wings, and the wings with prescribed deformation (green) under the gust from various directions shown on top of the panels
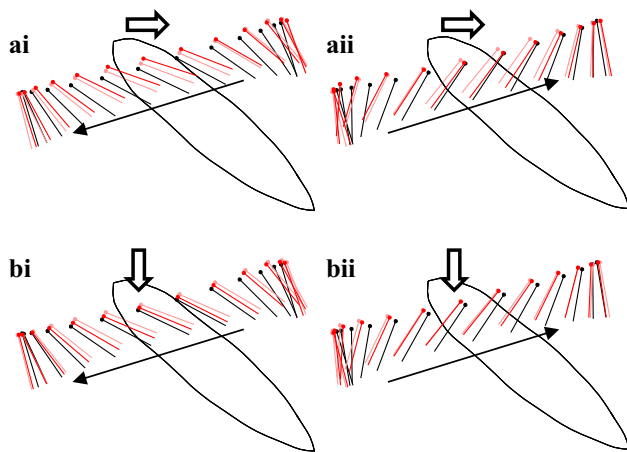

Fig. 12 Time-series of the wing cross sections of rigid (black) and flexible wings with (red) or without (pink). **a** Frontal ($\theta = 0°$) gust at 80% of wing length from wing base during (i) down-stroke, (ii) up-stroke. **b** Downward ($\theta = 90°$) gust at 80% of wing length from wing base during (i) down-stroke, (ii) up-stroke

moths use wing flexibility to mitigate the gust effect, but our results point out the importance of the flexible wing design of micro-air vehicles for the gust response.

5 Conclusion

In this study, we numerically investigated the gust response of a flapping wing flyer with flexible wings with the longitu-

dinal gust model that follows smoothed step function. Even though the effects are small compared with the conventional fixed wing aircraft as suggested previously, the aerodynamic forces on the flapping wings are affected by the gust from various directions. The passive wing deformation can reduce the force changes by responding to the gust except for the downward gust, because the flexibility allows the wings to change the wing shape favourable to the gust rejection adaptively. Such passive response of the flexible structure, and its capability to mitigate the gust, may facilitate the neural control in unpredictable environment. The results in this study, therefore, point out the great importance of the wing flexibility for micro-air vehicles in terms of its robustness under disturbances.

References

1. Watkins, S., Milbank, J., Loxton, B.J., et al.: Atmospheric winds and their implications for micro air vehicles. AIAA J. **44**, 2591–2600 (2006)
2. Combes, S.A., Dudley, R.: Turbulence-driven instabilities limit insect flight performance. Proc. Natl. Acad. Sci. USA **106**, 9105–9108 (2009)

3. Ravi, S., Crall, J.D., McNeilly, L., et al.: Hummingbird flight stability and control in freestream turbulent winds. J. Exp. Biol. **218**, 1444–1452 (2015)

4. Vance, J.T., Faruque, I., Humbert, J.S.: Kinematic strategies for mitigating gust perturbations in insects. Bioinspir. Biomim. **8**, 016004 (2013)

5. Fuller, S.B., Straw, A.D., Peek, M.Y., et al.: Flying Drosophila stabilize their vision-based velocity controller by sensing wind with their antennae. Proc. Natl. Acad. Sci. USA **111**, E1182–E1191 (2014)

6. Ravi, S., Crall, J.D., Fisher, A., et al.: Rolling with the flow: bumblebees flying in unsteady wakes. J. Exp. Biol. **216**, 4299–4309 (2013)

7. Ortega-Jimenez, V.M., Greeter, J.S.M., Mittal, R., et al.: Hawkmoth flight stability in turbulent vortex streets. J. Exp. Biol. **216**, 4567–4579 (2013)

8. Ortega-Jimenez, V.M., Sapir, N., Wolf, M., et al.: Into turbulent air: size-dependent effects of von Kármán vortex streets on hummingbird flight kinematics and energetics. Proc. R. Soc. B **281**, 20140180 (2014)

9. Ortega-Jimenez, V.M., Mittal, R., Hedrick, T.L.: Hawkmoth flight performance in tornado-like whirlwind vortices. Bioinspir. Biomim. **9**, 025003 (2014)

10. Ellington, C.P., van den Berg, C., Willmott, A.P., et al.: Leading-edge vortices in insect flight. Nature **384**, 626–630 (1996)

11. Dickinson, M.H., Lehmann, F.O., Sane, S.P.: Wing rotation and the aerodynamic basis of insect flight. Science **284**, 1954–1960 (1999)

12. Srygley, R.B., Thomas, A.L.R.: Unconventional lift-generating mechanisms in free-flying butterflies. Nature **420**, 660–664 (2002)

13. Bomphrey, R.J., Nakata, T., Phillips, N., et al.: Smart wing rotation and trailing-edge vortices enable high frequency mosquito flight. Nature **544**, 92–95 (2017)

14. Engels, T., Kolomenskiy, D., Schneider, K., et al.: Bumblebee in heavy turbulence. Phys. Rev. Lett. **116**, 028103 (2016)

15. Sun, M.: Insect flight dynamics: stability and control. Rev. Mod. Phys. **86**, 615–646 (2014)

16. Liu, H., Ravi, S., Kolomenskiy, D., et al.: Biomechanics and biomimetics in insect-inspired flight systems. Philos. Trans. R. Soc. **B371**, 20150390 (2016)

17. Sane, S.P., Dickinson, M.H.: The control of flight force by a flapping wing: lift and drag production. J. Exp. Biol. **204**, 2607–2626 (2001)

18. Elzinga, M.J., Dickson, W.B., Dickinson, M.H.: The influence of sensory delay on the yaw dynamics of a flapping insect. J. R. Soc. Interface **9**, 1685–1696 (2012)

19. Wootton, R.J.: Support and deformability in insect wings. J. Zool. **193**, 447–468 (1981)

20. Combes, S.A., Daniel, T.L.: Into thin air: contributions of aerodynamic and inertial-elastic forces to wing bending in the hawkmoth *Manduca sexta*. J. Exp. Biol. **206**, 2999–3006 (2003)

21. Nakata, T., Liu, H.: Aerodynamic performance of a hovering hawkmoth with flexible wings: a computational approach. Proc. R. Soc. **B279**, 722–731 (2012)

22. Young, J., Walker, S.M., Bomphrey, R.J., et al.: Details of insect wing design and deformation enhance aerodynamic function and flight efficiency. Science **325**, 1549–1552 (2009)

23. Du, G., Sun, M.: Effects of wing deformation on aerodynamic forces in hovering hoverflies. J. Exp. Biol. **213**, 2273–2283 (2010)

24. Zheng, L., Hedrick, T.L., Mittal, R.: Time-varying wing-twist improves aerodynamic efficiency of forward flight in butterflies. PLoS ONE **8**, e53060 (2012)

25. Le, T.Q., Truong, T.V., Park, S.H., et al.: Improvement of the aerodynamic performance by wing flexibility and elytra–hind wing interaction of a beetle during forward flight. J. R. Soc. Interface **10**, 20130312 (2013)

26. Dickinson, M.H., Farley, C.T., Full, R.J., et al.: How animals move: an integrative view. Science **288**, 100–106 (2000)

27. Kubow, T.M., Full, R.J.: The role of the mechanical system in control: a hypothesis of self-stabilization in hexapedal runners. Philos. Trans. R. Soc. Lond. **B354**, 849–861 (1999)

28. Carruthers, A.C., Thomas, A.L.R., Taylor, G.K.: Automatic aeroelastic devices in the wings of a steppe eagle *Aquila nipalensis*. J. Exp. Biol. **210**, 4136–4149 (2007)

29. Ravi, S., Kolomenskiy, D., Engels, T., et al.: Bumblebees minimize control challenges by combining active and passive modes in unsteady winds. Sci. Rep. **6**, 35043 (2016)

30. Mistick, E.A., Mountcastle, A.M., Combes, S.A.: Wing flexibility improves bumblebee flight stability. J. Exp. Biol. **219**, 3384–3390 (2016)

31. Chen, J.S., Chen, J.Y., Chou, Y.F.: On the natural frequencies and mode shapes of dragonfly wings. J. Sound Vib. **313**, 643–654 (2008)

32. Ha, N.S., Truong, Q.T., Goo, N.S., et al.: Relationship between wingbeat frequency and resonant frequency of the wing in insects. Bioinspir. Biomim. **8**, 046008 (2013)

33. Nakata, T., Liu, H.: A fluid-structure interaction model of insect flight with flexible wings. J. Comput. Phys. **231**, 1822–1847 (2012)

34. Liu, H.: Integrated modeling of insect flight: from morphology, kinematics to aerodynamics. J. Comput. Phys. **228**, 439–459 (2009)

35. Willmott, A.P., Ellington, C.P.: The mechanics of flight in the hawkmoth *Manduca sexta*. I. kinematics of hovering and forward flight. J. Exp. Biol. **200**, 2705–2722 (1997)

36. Nakata, T., Liu, H.: A fluid-structure interaction model of insect flight with flexible wings. J. Comput. Phys. **231**, 1822–1847 (2012)

37. Sun, M., Xiong, Y.: Dynamic flight stability of a hovering bumblebee. J. Exp. Biol. **208**, 447–459 (2005)

38. Taylor, G.K., Thomas, A.L.R.: Animal flight dynamics II. Longitudinal stability in flapping flight. J. Theor. Biol. **214**, 351–370 (2002)

39. Viswanath, K., Tafti, D.K.: Effect of frontal gusts on forward flapping flight. AIAA J. **48**, 2049–2062 (2010)